Volume 302, number 1, 21–25 FEBS 10975 May 1992

Level of expression controls modes of gating of a K^+ channel

Ofira Moran[a], Wolfgang Schreibmayer[b], Lukas Weigl[b], Nathan Dascal[a] and Ilana Lotan[a]

[a]*Department of Physiology and Pharmacology, Sackler School of Medicine, Tel Aviv University, Ramat Aviv 69978, Israel* and [b]*Institute of Medical Physics and Biophysics, Karl-Franzens University Graz, A-8010 Graz, Austria*

Received 28 January 1992; revised version received 11 March 1992

Several distinct subfamilies of K^+ channel genes have been discovered by molecular cloning, however, in some cases the structural differences among them do not account for the diversity of K^+ current types, ranging from transient A-type to slowly inactivating delayed rectifier-type, as members within each subfamily have been shown to code for K^+ channels of different inactivation kinetics and pharmacological properties. We show that a single K^+ channel cDNA of the *Shaker* subfamily (*Sh*H4) can express in *Xenopus* oocytes not only a transient A-type K^+ current but also, upon increased level of expression, slowly inactivating K^+ currents with markedly reduced sensitivity to tetraethylammonium. In correlation with the macroscopic currents there are single-channel gating modes ranging from the fast-inactivation mode which underlies the transient A-type current, to slow-inactivation modes characterized by bursts of longer openings, and corresponding to the slowly inactivating macroscopic currents.

Potassium channel; cDNA expression; *Xenopus* oocyte; Single-channel analysis; Inactivation kinetics

1. INTRODUCTION

Voltage-dependent K^+ channels comprise a diverse family of ion channels which are important in excitability of neurons and muscles and in some aspects of synaptic transmission [1,2]. Four distinct subfamilies of K^+ channel genes were isolated originally from *Drosophila* (e.g. [3,4]) and later, mammalian counterparts for each subfamily were isolated as well [5]. Although members of a given subfamily are highly homologous in their primary sequence, when expressed in *Xenopus* oocytes, they display K^+ currents of diverse voltage sensitivity and kinetic properties ranging from rapidly inactivating A-type currents to slowly inactivating delayed rectifier-type currents. Notably, of the *Shaker* subfamily members isolated from *Drosophila*, all but one carry fast transient A-type currents, while in mammalian members of this subfamily, all but one carry slowly inactivating delayed rectifier-type currents. Also, the sensitivity to pharmacological agents varies among members of the same group [6–12]. In fact, it is not always possible to predict the type of the current from the primary amino acid sequence. Most intriguing was when two different research groups expressed in the oocytes of the same predicted amino acid sequence channels, yet recorded whole cell currents of either A-type [10] or delayed rectifier-type [13].

One of the *Drosophila* clones, *Shaker* H4 (*Sh*H4 [8]; almost identical to *Sh*B [7]), was reported to direct transient A-type current in *Xenopus* oocytes injected with its cRNA. In this report we demonstrate that this cRNA, derived from single cDNA, leads also, at very high doses, to the appearance in the oocytes of slowly inactivating macroscopic K^+ currents with different pharmacological properties. At the single-channel level there are not only channels with fast-inactivation mode, as described by Zagotta et al. [14], but also channels with slow-inactivation modes of increased open duration and number of openings per burst. We show that the factor inducing the slow kinetics is an increased level of expression of channels encoded by this cDNA and propose possible mechanisms.

Correspondence address: I. Lotan, PO Box 39048, Ramat-Aviv 61390, Israel. Fax: (972) (3) 6409113.

2. EXPERIMENTAL

Oocytes were prepared, injected and incubated as described [15,16]. In brief, stage 5 and 6 oocytes were defolliculated by 3–4 h incubation with collagenase (1.5 mg/ml in Ca^{2+}-free ND96 solution: 96 mM NaCl, 2 mM KCl, 1 mM $MgCl_2$, 5 mM HEPES, pH 7.5) and then transferred to ND96 solution with 1.8 mM $CaCl_2$ and 2.5 mM sodium pyruvate, 100 μg/ml streptomycin and 100 U/ml penicillin and injected with different concentrations of cRNA. The cRNA was generated from a recombinant Bluescript plasmid containing the *Sh*H4 cDNA (a gift from Mark Tanouye) as described [17] and was determined by agarose gel electrophoresis to be pure. Currents were assayed electrophysiologically after one-to-several days incubation in this medium.

Electrophysiological recordings of macroscopic currents were performed at 21–23°C using a two-electrode voltage clamp technique as described [18]. The electrode resistance was 0.5–2 MΩ. In all experiments the currents and the voltage were monitored simultaneously and traces with voltage deviations of more than 2 mV were discarded. Series resistance was not compensated for. The holding potential was −80 mV and the currents were elicited by depolarizing pulses to different voltages. The bath solution was ND96 supplemented with 1 mM $CaCl_2$. When desired, K^+ concentration was raised by replacing NaCl with KCl in the ND96 solution. To calculate the net K^+ current, leak currents elicited at voltages where the K^+ current was not yet apparent were measured, averaged, scaled up and subtracted from the total current at each voltage. No off-line capacity transient correction was

made. After 40 ms at a membrane voltage of 0 mV, usually an outward Ca-dependent Cl^- current of 40–200 nA developed. In most cases, 1 mM of 9-antracenecarboxylic acid was added to the ND96 solution to reduce this current to below 50 nA [18,19].

Patch-clamp recordings [20] at 18–20°C and data acquisition were performed in cell-attached configuration as described [21]. Single-channel currents were filtered at 2 kHz (four-pole Bessel), digitized at 10 kHz and digitally filtered at 1 kHz [21]. The resting potential was zeroed by the extracellular solution containing (mM): K^+/glutamate 58.5, KCl 37.5, $CaCl_2$ 1, $MgCl_2$ 1, glucose 10 and HEPES/K^+ 10, pH 7.4. In the pipette (Sylgard-coated hard and soft glasses, resistance 0.7–13 MΩ) was (mM): NaCl 96, KCl 2, $MgCl_2$ 2, $CaCl_2$ 2 and HEPES/Na^+ 10, pH 7.4. Data were analyzed with pClamp 5.5.1 software (Axon Instr., USA) as described [21]. For assessment of burst duration, closed-time distributions were fitted with double exponential functions. Closed times ≤ 3 × the fast-time constant were considered as short closures within a burst and the others as interburst closures.

P values were calculated using the two-tailed *t*-test. Values are presented as mean ± S.E.M. (number of oocytes).

3. RESULTS

3.1. *Macroscopic currents through* Sh*H4 channels display different inactivation patterns and pharmacological profile*

When we and others [7,8,17,22] expressed A-type currents from *Sh*H4 and *Sh*B in oocytes, usually the concentration of the injected cRNA did not exceed 10 ng/oocyte. The current elicited by a depolarizing pulse lasting for several tens of milliseconds was assayed by the two-electrodes voltage clamp technique and displayed two components: a major transient component, declining with a time constant of several milliseconds, an a sustained component, remaining at the end of the pulse. The fraction of the sustained current was about 0.1 to 0.2 of the peak at 0 mV (e.g. see Fig. 2A; the sustained component probably represents re-openings of single-channels from a non-absorbing state, see [14,22]). However, we have noticed that in fact the kinetics of the current are 'maneuverable' depending on both the concentration of the cRNA injected and the number of days that elapsed since the injection. Fig. 1A demonstrates a typical example where different oocytes, taken from one donor and injected on the same day with different cRNA concentrations, exhibit currents of different inactivation patterns after three days. For further analysis the inactivation kinetics of the currents were quantified by measuring the total current (T = amplitude at the time of the peak) and the sustained current (S = amplitude at the end of a 40 ms pulse when the transient current is completely inactivated, see Fig. 2A) at 0 mV, and calculating the ratio S/T in all oocytes tested. Each macroscopic current was assigned to one of three groups of fast-, intermediate- and slow-inactivation, corresponding to S/T of < 0.3, 0.3–0.65, > 0.65, respectively. A plot of S/T as a function of the number of days after the injection and of cRNA concentration yields a histogram (Fig. 1B) which clearly reflects the trend that the fraction of the sustained current increases with increasing number of days and with cRNA concentration.

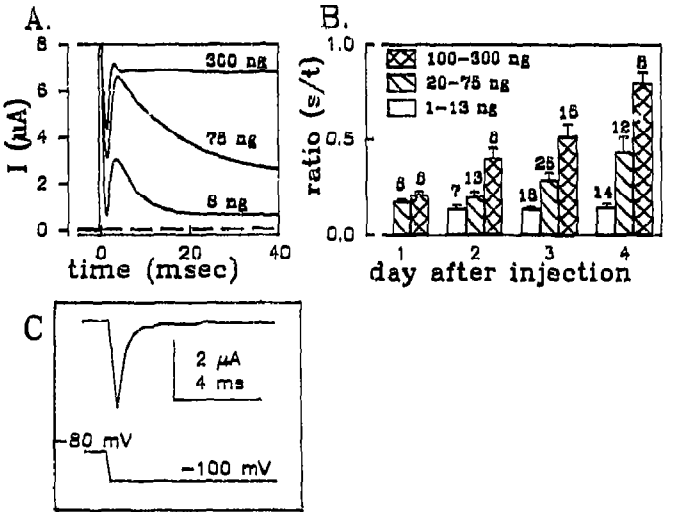

Fig. 1. (A) Patterns of K^+ currents in three oocytes of the same frog, assayed three days after injection of different amounts of *Sh*H4 cRNA (indicated above the traces). The dashed line represents the zero current level. The currents were recorded at 0 mV and the holding potential was −80 mV. The traces shown are leak subtracted. (B) A histogram reflecting the trend that kinetics of the currents depend on the cRNA concentration and number of days that elapsed since the injection. Unbalanced analysis of variance and co-variance with repeated measures (variance components) yield a statistically significant correlation between log S/T (S/T was not checked as it did not display normal distribution) and concentration ($P < 0.0001$) and number of days in each concentration group ($P < 0.0001$). Number of oocytes tested are shown above the bars. Amounts of injected cRNA per oocyte are indicated in the figure. (C) Current (upper trace) evoked by a hyperpolarizing pulse (bottom trace, actual membrane voltage) is shown to demonstrate actual capacity transient.

The absolute value of S/T for a given cRNA concentration and number of days varied among frogs.

The voltage-dependence of the currents in oocytes of the three groups was studied by eliciting the currents by steps to various depolarizing voltages from a holding potential of −80 mV (Fig. 2). Activation analysis in the three groups was done by fitting the data to modified Bolzmann equation (see [17]). The parameters of half-activation voltage and slope factor did not differ substantially among the three groups (not shown). However, the maximal conductance changed significantly; it was (in μS) 48.4 ± 6.2 (n=25), 137 ± 9.1 (n=27) and 153.6 ± 18 (n=12) in oocytes of fast-, intermediate- and slow-inactivation, respectively (P<0.0001 for the difference between fast- and slow-inactivation). The reversal potentials of the fast- and slow-inactivating currents were similar in 2 mM extracellular K^+: −78 ± 7.1 mV (n=27) and −81 ± 3.6 mV (n=12), respectively (determined from the fit to Bolzmann exuation), and were also similar in 96 mM extracellular K^+: −1.3 ± 2.7 mV (n=4) and −4.7 ± 0.6 mV (n=3), respectively (determined directly from the I–V curve). Thus, the ionic nature of the fast- and slow-inactivating currents is similar, with both currents carried mainly by K^+ ions.

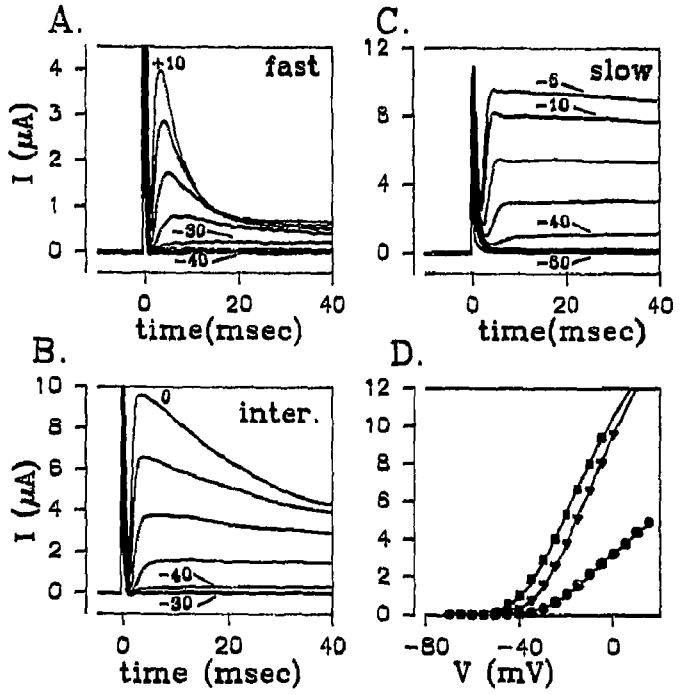

Fig. 2. Voltage-dependence of activation of K^+ macroscopic currents expressed from *Sh*H4 cRNA in representative oocytes of each of the three groups. (A–C) Families of currents evoked by depolarizing voltage steps to the indicated voltages from a holding potential of −80 mV in normal ND96 solution (2 mM K^+). The first step was to −70 mV and the increment between successive steps was 5 mV. (Traces with increments of 10 mV are shown). Currents were corrected for leak in all oocytes. (D) Current–voltage relationships of fast- (●), intermediate- (▼) and slow- (■) inactivating currents. Ordinate, current in μA.

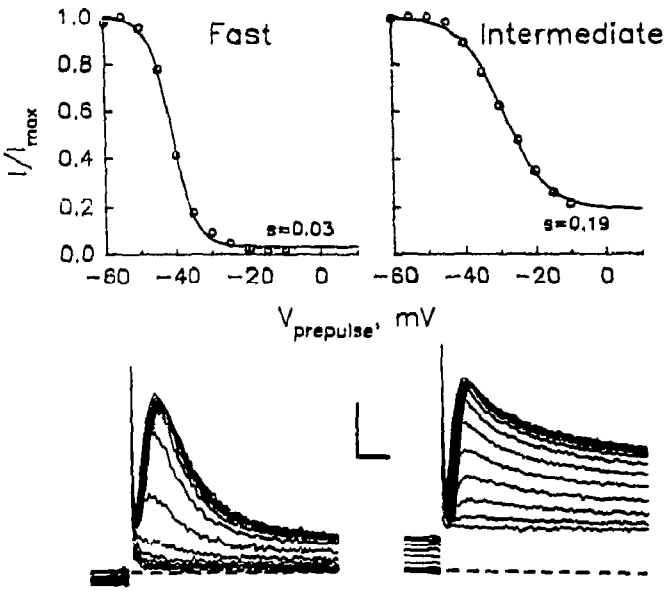

Fig. 3. Voltage-dependence of inactivation of macroscopic K^+ currents expressed in two oocytes of fast- (left panel) and intermediate-inactivation (right panel). Steady-state inactivation was assessed by holding the cell at −80 mV and stepping the voltage to various prepulses ($V_{prepulses}$) for 2.5 s and then measuring the current elicited by a step to 0 mV. Currents elicited with prepulses of −100 to −10 mV with 5 mV intervals are shown in the lower traces. The dashed line shows the calculated zero current at 0 mV. Normalized currents were fitted to Boltzmann distribution (upper traces) assuming the existence of a single inactivation gate and a fraction of current which does not inactivate, using the equation:

$$I/I_{max} = (1 + s)/\{1 + \exp[(V_{prepulses} - V_h)/a_h] + s\}$$

where I_{max} is the current obtained by the step from −80 mV, s is the fraction of the current that does not inactivate by 2.5 s prepulse in the range of prepulse voltages applied, and the parameters V_h (half-inactivation voltage) and a_h (slope factor) were allowed to change in wide ranges. The parameters for the oocytes of fast- and intermediate-inactivation shown were V_h (mV) = −41.1 and −28.9, a_h (mV) = 3.31 and 6.0, respectively. s values are denoted in the figure. Calibration bars: horizontal, 6 ms; vertical, 600 or 3,000 nA for the fast- or the intermediate-inactivating currents, respectively.

The voltage-dependence of inactivation of the currents was studied by analysis of their steady-state inactivation curves (Fig. 3). Most noticeably, the fraction of the non-inactivating component in the current trace (s in the fitting procedure, see legend to Fig. 3) changed significantly among the groups. The non-inactivating current was a minor component (s=0.069 ± 0.015, n=9) of fast-inactivating currents and became the dominant component (s=0.6 ± 0.084, n=4) of slow-inactivating currents.

K^+ channel blockers were tested to assess the pharmacological properties of the different currents. While fast- and slow-inactivating currents were about equally sensitive to 4-aminopyridine (IC_{50} ~1 mM) their sensitivity to tetraethylammonium (TEA) was different. 50 mM TEA blocked fast-inactivating currents by 77 ± 1% (n=4) and slow-inactivating currents by only 21 ± 4% (n=7); the difference in sensitivity was statistically significant (P<0.001).

3.2. *Single-channel modes of fast- and slow-inactivation underlie the macroscopic currents*

Currents from oocytes (n=19), previously tested by two-electrode voltage clamp, were also recorded from cell-attached patches (n=24) containing between 1 and 4 channels. Detailed analysis of 13 of these patches containing either 1 or 2 channels revealed that, besides channels with 'normal' *Sh*H4 fast-inactivation mode characterized by few rapid openings with short mean open-time that appeared following depolarization [14]; see Fig. 4A, left panel), channels with slow-inactivation modes could also be observed (see Fig. 4A, right panel). The slow-inactivation modes were characterized by prolonged bursting behavior with larger mean open-time. We measured the S/T ratio of each ensemble-averaged patch current (S/T_p), and called the channels with S/T_p<0.2 fast-inactivating and those with S/T>0.2 slow-inactivating. The slow-inactivating channels displayed various inactivation kinetics (various S/T_p values) resembling those of the intermediate- and slow-inactivating macroscopic currents. The single-channel current amplitudes at 0 mV were the same for the fast-inactivating (0.51 ± 0.03 pA; n=4) and for the slow-inactivating

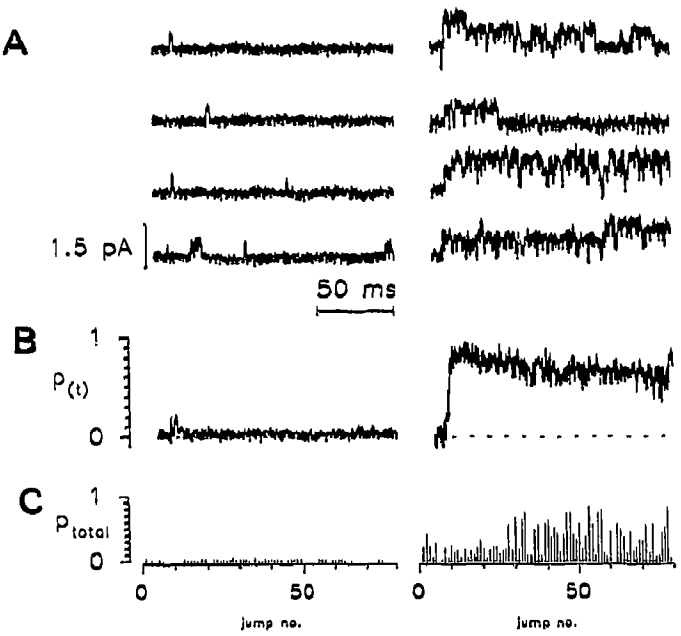

Fig. 4. (A) Fast- (left panel) and slow- (right panel) inactivating single-channel openings elicited by a depolarizing pulse of 150 ms duration to 0 mV from a holding potential of −80 mV. (B) Open probability (p_t) for the single-channel records shown in (A), calculated by averaging 80 (left) and 64 (right) current traces and dividing by the number of channels (n=1 and n=2 for the fast and the slow patches shown, respectively) and the single-channel current amplitudes at 0 mV (see text). Time scales are as in (A). (C) Total open probability (p_{total}) of fast- (left) en slow- (right) inactivating patches, calculated for the 150 ms depolarizing pulse to 0 mV (same patches as in A).

channels (0.53 ± 0.02 pA; n=4). Peak open probability ($p_{(o)}$) of the slow-inactivating channels was considerably higher as evidenced directly from Fig. 4B (patches with S/T_p<0.2 had $p_{(o)}$ of 0.21 ± 0.05, n=5, whereas those with S/T_p>0.3 had $p_{(o)}$ of 0.75 ± 0.15, n=6; P<0.001). Accordingly, also total open probability, calculated for the whole voltage pulse, was drastically increased in slow-inactivating channels (Fig. 4C).

In these 13 patches a slow-inactivating channel was never found alone in a patch, but was always accompanied by another one or more channels of the same conductance (in one patch, in addition to a slow-inactivating channel, there was a second channel of small conductance which was interpreted as a 'rim' channel). The fast-inactivating channels appeared to occur singly in certain patches; however, because of the transient nature of their openings, the presence of more than one channel could not be definitely excluded.

In all of the 24 patches (of 1–4 channels) recorded, the patches with fast-inactivating ensemble-averaged currents were encountered in oocytes of both fast- and slow-inactivation. The patches with slow-inactivating ensemble-averaged currents appeared more frequently in oocytes of the slow-inactivation group (the proportion of these patches was 38%: 6 out of 16 with mean S/T_p ratio of 0.51 ± 0.24) than in oocytes of the fast-inactivation group (the proportion was 25%: 2 out of 8 had S/T_p ratios of 0.56 and 0.33). Thus, the frequency of encountering slow-inactivating channels is higher in oocytes having slow-inactivating macroscopic currents.

4. DISCUSSION

We have demonstrated that a single species cRNA can direct macroscopic K^+ currents differing in their inactivation kinetics (ranging from transient to non-inactivating) as well as in their sensitivity to TEA. The slow-inactivating currents are brought about by increased cRNA concentration and/or number of days during which the channels are expressed. At the molecular level, there are not only the channels of fast-inactivation mode which carry the macroscopic transient current [14], but also channels of slow-inactivation mode with similar unitary conductance.

The channels of slow-inactivation display ensemble-averaged currents resembling the various slow-inactivating macroscopic currents. Thus, it seems reasonable that the channels of slow-inactivation underlie the slow macroscopic kinetics. However, although these channels were encountered more frequently in oocytes of the slow-inactivation group, their proportion of total channels was still only 38% in these oocytes. In the following we show that, despite this apparent small proportion, the slow- inactivating channels can still generate most of the macroscopic slow-inactivating currents. Firstly, the probability that the slow-inactivating channels are open at the time of the peak is about 4-times higher than that of the fast-inactivating channels, and is even higher during the rest of the depolarizing pulse. Thus, each slow-inactivating channel contributes more to the macroscopic current than a fast-inactivating channel. Secondly, our observation that the slow-inactivating channels were never detected alone in a patch may be an indication that they tend to cluster, thereby reducing the probability of encountering them in a patch, at least by a factor of two (assuming a minimal cluster of two channels). Taken together, in an oocyte in which fast- and slow- inactivating channels contribute equally to the peak current, one should encounter patches of fast- and slow- inactivation at a ratio of about 1:8. In fact, in oocytes of the slow-inactivation group the ratio was better, 1:2.7 (38%). Thus, based on this calculation the slow-inactivating channels contribute more than the fast-inactivating ones to the peak current of slow-inactivating macroscopic currents, and carry practically all this current during the rest of the depolarizing pulse. However, extensive statistics are needed for the confirmation of this argument.

The distinct components of the macroscopic current and the different single channel modes suggest that there are some channel structures whose functions have changed. Since the fast-inactivation rate is strikingly affected, the N-terminus is the most likely candidate as

it plays an important role in the fast-inactivation of this channel [23]. Indeed, the characteristics of the slow-inactivation modes resemble closely the effects of mutations in this region that eliminate the fast inactivation [23]. Alterations in N-terminus can probably account also for the diverse TEA sensitivity, as it was shown [24] that two members of the *Shaker* subfamily, differing only in their N-terminals, direct two different currents, with respect to kinetics and TEA sensitivity, resembling the transient and sustained currents demonstrated by us.

Since the currents with slow-inactivation kinetics are induced upon increased level of functional channel expression, as indicated by the large maximal conductances, we propose two plausible mechanisms whereby the modification in the N-terminal may occur. One mechanism is based upon our observation that the slow-inactivating channels tend to appear in groups, a tendency which was not observed for the fast-inactivating channels [14,23]. Upon increased synthesis, tetrameric channels [25] may cluster, possibly through interactions of N-terminals, leading to impaired functioning of the 'ball and chain' [23,26] without affecting the single-channel conductance. The varying modes of opening may imply different degrees of interaction between adjacent tetrameric channels and different numbers of tetrameric channels forming a cluster. The second possible mechanism is that the slow-inactivating channels are differentially processed or modified in the N-terminus due to intracellular changes (e.g. depletion of endogenous factors) caused by the 'mass production' of functional channels. An N-terminal cysteine in position 13 of A-type channels, RCK4, from rat brain expressed in *Xenopus* oocytes [9] was recently found to be responsible for fast-to-slow mode interconversion after patch excision [27]. No such cysteine is, however, present in *Sh*H4 clone and therefore cannot account for the observed behavior.

*Sh*H4 is a representative of a K^+ channel gene subfamily which also has neuronal members, and we therefore suggest that gene expression could serve as a potent modulator of K^+ channel behavior in neurons and synapses. Constitutive expression of different levels of A-type channels in different neurons could underlie the varying relations of the observed A-type channel modes in neurons, thus determining neuron excitability [28]. Induced expression of A-type channels in a given neuron or synapse could serve as a mechanism for facilitated inhibition, since the outward current will not only increase in amplitude, but it will also last longer and will be elicited by smaller depolarization.

Acknowledgements: We thank Rafi Korenstein for reviewing the manuscript and Martin Wallner for sequence alignment of different K^+ channels. This study has been supported by the USA–Israel Binational Science Foundation, the Israel Academy of Sciences, Austrian Research Foundation (project S4505B) and the Karl-Franzens University, Graz (fellowship to N.D.).

REFERENCES

[1] Hille, B. (1984) Ionic Channels of Excitable Membranes, Sinauer Associates, Sunderland MA.
[2] Rudy, B. (1988) Neuroscience 25, 729–750.
[3] Tempel, B., Papazian, D.M., Schwartz, T.L., Jan, Y.N. and Jan, L.Y. (1987) Science 237, 770–775.
[4] Butler, A., Wei, A., Baker, K. and Salkoff, L. (1989) Science 243, 943–947.
[5] Stuhmer, W. (1991) Annu. Rev. Biophys. Chem. 20, 65–78.
[6] Timpe, L.C., Jan, Y.N. and Jan, L.Y. (1988) Neuron 1, 659–667.
[7] Timpe, L.C., Schwarz, T.L., Tempel, B.L., Papazian, D.M., Jan, Y.N. and Jan, L.Y. (1988) Nature 331, 143–145.
[8] Iverson, L.E., Tanouye, M.A., Lester, H.A., Davidson, N. and Rudy, B. (1988) Proc. Natl. Acad. Sci. USA 85, 5723–5727.
[9] Stuhmer, W., Ruppersberg, J.P., Hasso, K., Sakmann, B., Stocker, M., Giese, K.P., Perschke, A., Baumann, A. and Pongs, O. (1989) EMBO J. 8, 3235–3244.
[10] Christie, M.J., Adelman, J.P., Douglass, J. and North, R.A. (1989) Science 244, 221–224.
[11] Baumann, A., Grupe, A., Ackerman, A. and Pongs, O. (1988) EMBO J. 7, 2457–2463.
[12] Kirsch, G.E., Drewe, J.E., Verma, S., Brown, A.M. and Joho, R.H. (1991) FEBS Lett. 278, 55–60.
[13] Stuhmer, W., Stocker, M., Sackmann, B., Seeburg, P., Baumann, A., Grupe, A. and Pongs, O. (1988) FEBS Lett. 242, 199–206.
[14] Zagotta, W.N., Hoshi, T. and Aldrich, R.W. (1989) Proc. Natl. Acad. Sci. USA 86, 7243–7247.
[15] Dascal, N., Landau, E.M. and Lass, Y. (1984) J. Physiol. 352, 551–574.
[16] Dascal, N. and Lotan, I. (1991) Neuron 6, 165–175.
[17] Moran, O., Dascal, N. and Lotan, I. (1991) FEBS Lett. 279, 256–259.
[18] Lotan, I., Volterra, A., Dash, P., Siegelbaum, S.A. and Goelet, P. (1988) Neuron 1, 963–971.
[19] Botton, R., Dascal, N., Gillo, B. and Lass, Y. (1989) J. Physiol. 408, 511–534.
[20] Hamil, O.P., Marty, A., Neher, E., Sackmann, B. and Sigworth, F.J. (1981) Pflügers Arch. 391, 85–100.
[21] Schreibmayer, W., Dascal, N., Lotan, I., Weigl, L. and Wallner, M. (1991) FEBS Lett. 291, 341–344.
[22] Iverson, L.E. and Rudy, B. (1990) J. Neurosci. 10, 2903–2916.
[23] Hoshi, T., Zagotta, W. and Aldrich, R.W. (1990) Science 250, 533–538.
[24] Stocker, M., Stuhmer, W., Wittka, R., Wang, X., Muller, R., Ferrus, A. and Pongs, O. (1990) Proc. Natl. Acad. Sci. USA 87, 8903–8907.
[25] MacKinnon, R. (1991) Nature 350, 232–235.
[26] Zagotta, W.N., Hoshi, T. and Aldrich, R.W. (1990) Science 250, 568–571.
[27] Ruppersberg, J.P., Stocker, M., Pongs, O., Heinemann, H., Frank, R. and Koenen, M. (1991) Nature 352, 711–714.
[28] Cooper, E. and Shrier, A. (1989) J. Gen. Physiol. 94, 881–910.